Korean J. Chem. Eng., **24**(6), 965-974 (2007)

Characterization of metal (Ba, Al, Si, V, and W)-incorporated TiO_2 and toluene photodecomposition in the presence of H_2O

Seong-il Yoon, In-Gyung Jung* and Misook Kang,†**

Department of Life Science, College of Natural Sciences, Hanyang University, Seoul 133-791, Korea
*Research Institute of Industrial Science & Technology (RIST), Pohang, Gyeongbuk 790-600, Korea
**Department of Chemistry, College of Science, Yeungnam University, Gyeongsan, Gyeongbuk 712-749, Korea
(*Received 29 May 2007 • accepted 28 June 2007*)

Abstract−This study focused on toluene photodecomposition in the presence of H_2O over metal (Ba, Al, Si, V, and W)-incorporated TiO_2. The nanometer-sized, metal-TiO_2 photocatalyst samples, including Ba^{2+}, Al^{3+}, Si^{4+}, V^{5+}, and W^{6+} ions, were prepared by using the solvothermal method. The X-ray photoelectron spectroscopy (XPS) results showed that the Ti-OH peak, which indicates hydrophilicity, increased with increasing Al and Si ion components but decreased with increasing Ba, V, and W ion components. The contact angles were distributed over the range of 0-10° on almost all films (200-nm thick) after irradiation for 2 h, and in particular approached 0° on the Al-TiO_2 and Si-TiO_2 nanometer-sized films after just 30 min. The toluene (100 ppm) photodecomposition in the continuous system increased in the order of Al-TiO_2>Si-TiO_2>pure TiO_2>W-TiO_2>Ba-TiO_2>V-TiO_2, and the maximum toluene conversion rate achieved was 45% over Al-TiO_2 film after 120 min. The toluene conversion remarkably increased; however, over all photocatalysts, with H_2O addition during the toluene photo-decomposed reaction, and in particular, the conversion reached up to 90% after 120 min over Al-TiO_2 and Si-TiO_2 with increased hydrophilicity. After photoreaction for 24 h, minimal carbon was deposited on the photocatalyst under both reaction conditions, with and without H_2O addition, although the deposited carbon amounts were smaller for the former. These results confirmed that the hydrophilicity of the photocatalyst had a greater effect on toluene decomposition, while the photocatalytic deactivation could be retarded by H_2O supplementation during toluene decomposition.

Key words: Solvothermal Method, Metal-TiO_2, Hydrophilicity, Toluene Decomposition, H_2O Addition

INTRODUCTION

A unique aspect of TiO_2 is that it actually has two distinct, photo-induced phenomena. The first is the well-known original photocatalytic phenomenon, which leads to the decomposition of organics. In this field, many studies have been done on the photocatalytic treatment of environmental pollutants using semiconductors like TiO_2. When a semiconductor made of TiO_2 absorbs a photon and then is promoted to an excited state, an electron is transferred from the valence band to the conduction band, where it can function as a reducing moiety, thereby leaving a hole in the valence band that becomes a strong oxidizing entity. The energy gap between the valence and conduction bands in pure TiO_2 is 3.2 eV, which necessitates the use of UV light to excite electrons on the TiO_2 surface. To activate the photocatalysts using UV light with longer wavelengths, many recent studies have focused on the doping/mixing of other sulfides or oxides, such as CdS, Fe_2O_3, ZnO, and SiO_2, which exhibit lower band gap energy, in the TiO_2 anatase structure [1-4].

The second photo-induced phenomenon, which is more recently discovered, is high wettability or "super-hydrophilicity." Depending on the composition and processing, the surface can have an increased photocatalytic and decreased super-hydrophilic character, or vice versa [5-8]. Super-hydrophilicity has recently attracted research attention. This effect was discovered by accident in 1995 at the laboratories of TOTO, Inc. It was found that if a TiO_2 film is prepared with a certain percentage of SiO_2, it acquires super-hydrophilicity after UV illumination [9,10]. The electrons reduce the Ti(IV) state to the Ti(III) state, and the resulting holes oxidize the O^2 anions. In the process, oxygen atoms are ejected, and oxygen vacancies are created which are occupied by water molecules, thereby producing adsorbed OH groups that tend to make the surface hydrophilic. The longer that the surface is illuminated with UV light, the smaller the contact angle for water becomes. Finally, under a moderate UV light intensity after 30 min, the contact angle approaches zero, with the result that water tends to spread perfectly across the surface.

More recently, many researchers have tried to develop a semiconductor material with an excellent self-cleaning (super-hydrophilic) property and high VOC decomposition. They expected that the clean surface of substrate-coated TiO_2 can be maintained forever if the radiation source and water are continually supplied, and that, in addition, it can simultaneously remove harmful organic pollutants that are attached on substrate-coated TiO_2. Until now, however, the developed materials have not completely satisfied the researchers due to the recovery of the hydrophobic property in dark conditions or longer rainy season, which decreases the hydrophilic activity and the VOC removal rate on the TiO_2 surface.

On the other hand, it has already been reported that H_2O stably and continuously functions as an OH radical donor in photoreaction with Fe/TiO_2. Too much H_2O addition, however, generates structural damage, which causes fast catalytic deactivation [11,12]. The relationship between the hydrophilicity (OH radical donor) of the photocatalyst and VOC decomposition with H_2O addition, however, is not yet clear. Some papers have reported that H_2O addition

†To whom correspondence should be addressed.
E-mail: mskang@ynu.ac.kr

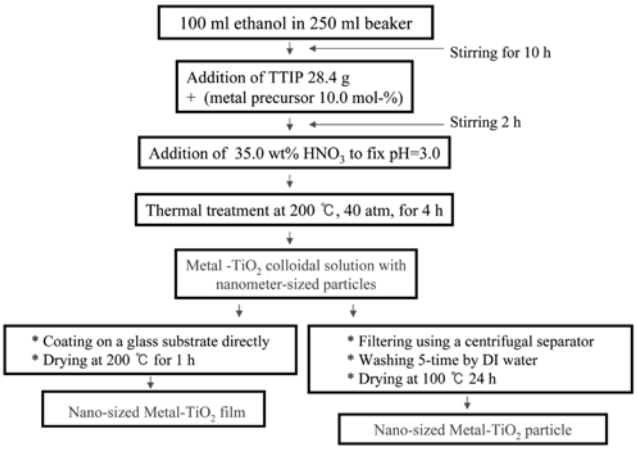

Fig. 1. Preparation of particles and films of metal-incorporated TiO_2 photocatalysts by the solvothermal method.

during photoreaction was not affected by photo-degradation [13,14]. This confirms that if the effect of super-hydrophilicity of the photocatalyst in VOC decomposition could be resolved, the application of the TiO_2 photocatalyst could be extended to various scientific fields.

This study attempted to determine firstly the hydrophilicity attained by the incorporation of various metals (Ba^{2+}, Al^{3+}, Si^{4+}, V^{5+}, and W^{6+} ions) into the TiO_2 anatase framework, secondly the relationship between the hydrophilicity of the photocatalyst and toluene decomposition ability with or without H_2O addition, and finally, the role of H_2O during toluene photodecomposition. The solvothermal method was used to prepare the following nano-sized metal oxides: Ba-TiO_2, Al-TiO_2, Si-TiO_2, V-TiO_2, and W-TiO_2.

EXPERIMENTAL

1. The Preparation of Metal-TiO_2 Photocatalysts

The commonly used solvothermal method was applied [15] as shown in Fig. 1. The reagents used for the preparation of the sol-mixture were titanium tetra-isopropoxide (99.95%), barium(II) chloride (99.9%), aluminum(III) isopropoxide (99.9%), tetra-ethyl-ortho silicate (99.9%), vanadium(VI) chloride (99.9%), and tungsten(VII) chloride (99.9%), all supplied by Junsei Chemical, Japan, which were used as Ti^{4+}, Ba^{2+}, Al^{3+}, Si^{4+}, V^{5+}, and W^{6+} precursors, respectively. The metal precursors were mixed with ethyl alcohol (99%, Wako Pure Chem., Ltd) in a beaker. The added metal precursors were fixed to 10.0 mol% per titanium precursor in gel mixtures. The pH value in the final solution was fixed to 3. The solution was transferred to an autoclave (model R-211, Reaction Engineering Inc., Korea), which was heated to 200 ºC at a rate of 10 ºC/min and held for 24 h. During thermal treatment, titanium and the other metals were hydrolyzed by the OH group in the solvent, and then the nanometer-sized, metal-TiO_2 crystals were formed by their condensation reaction. The colloidal solutions produced with the nanometer-sized, metal-TiO_2 particles were directly used to coat the glass substrates to obtain metal-TiO_2 films, which were then dried at 200 ºC for 24 h to remove any remaining alcoholic solvents.

The hydrophilicity on the TiO_2 film is increased with increasing film thickness. In general, the films made by TiO_2 particles using proper binder additives were very thick and turbid, suggesting that the film had increased hydrophilicity. However, we discovered that the hydrophilicity was just close to wetness rather than being pure hydrophilicity. Therefore, we used the solvothermal method to obtain thinner and very transparent films, with the final result of a 200-nm thick transparent film. On the other hand, the produced colloidal solutions were separated into a precipitation and a solution by centrifugation. The separated particles were washed and dried at 100 ºC for 24 h to identify their various physical properties.

2. Characterization of Synthesized Metal-TiO_2 Photocatalysts

The synthesized samples, Ba-TiO_2, Al-TiO_2, Si-TiO_2, V-TiO_2 and W-TiO_2 nanometer-sized powders, were identified through powder X-ray diffraction analysis (XRD, model PW 1830 from Philips) with nickel filtered Cu$K\alpha$ radiation (30 kV, 30 mA) at 2-theta angles from 5 to 70 degrees. The scan speed was 10 degrees/min and the time constant was 1.0 second. The particle size and shape of the powders were observed through scanning electron microscopy (SEM and FESEM, model JEOL-JSM35CF) with a power setting of 15.0 kV. The UV-visible spectrum was obtained by using a Shimadzu MPS-2000 spectrometer with a reflectance sphere. The special range was from 200 to 700 nm.

The sample's Brunauer, Emmett and Teller (BET) surface area and pore size distribution were measured through nitrogen gas adsorption in a continuous flow method by using a chromatograph equipped with a TCD detector at liquid nitrogen temperature (8 ºK). A mixture of nitrogen and helium was flowed as the carrier gas with the GEMINI2375 model from Micrometrics. The sample was thermally treated at 350 ºC for 3 h before nitrogen adsorption.

X-ray photoelectron spectroscopy (XPS, PHI 5700, PHI Com.) was used to analyze the binding energy between Ti2p, O1s and C1s. For measurement, fresh photocatalysts were pelletized with 1.0 mm, and then treated in vacuum overnight. The Al mono (pass energy= 23.5 eV) was used as X-ray source at 350 W power, 15 kV, and pressure of below 2.7×10^{-6} Pa during the measurement.

Photoluminescence (PL) spectroscopy measurements were also taken to examine the number of photo-excited electron hole pairs for all samples. Samples of 1.0 mm pellet type were measured at room temperature and liquid nitrogen temperature (8 ºK) using a He-Cd laser source of 325 nm.

3. H_2O-Temperature Programmed Desorption (TPD)

The activation energies for dehydration in catalysts were determined with a differential scanning calorimeter (DSC) equipped with a micro thermo-differential and gravimetric analyzer (Perkin Elmer Co., USA). A weight of 20 mg α-alumina was used as the reference sample. To keep the moisture conditions identical, the sample was analyzed after contacting with saturated NH_4Cl solution for 24 h. The Ozawa method presented a useful equation to calculate the activation energy for hydration of various thermal reactions based on the shifts of the maximum deflection temperature (T_m) of DSC thermo-grams upon the changing of heating rates [16].

$$\text{Log } \phi + 0.4567E/RT_m = \text{constant}$$

Here, ϕ is the heating rate, E the activation energy, and R the gas constant. The activation energy can be derived from the slope, 0.4567E/R, of the plot of log ϕ verse $1/T_m$. This experimental value has often been used to discuss the hydrophilic property of a structure. In this study, the activation energies for dehydration were determined with

this method.

4. Hydrophilicity on Meta-TiO_2 Photocatalyst Films

The 200-nm thick metal-TiO_2 (0.002 g) films were prepared via the solvothermal treatment as the metal-TiO_2 solution was directly fixed on a Pyrex glass substrate as shown in Fig. 2. The hydrophilicity was evaluated by measuring the changes in the contact angle of water droplets at 298 K after UV-irradiation (model UV-A, 365 nm, 6.0 W/cm^2). The contact angle was measured with a commer-

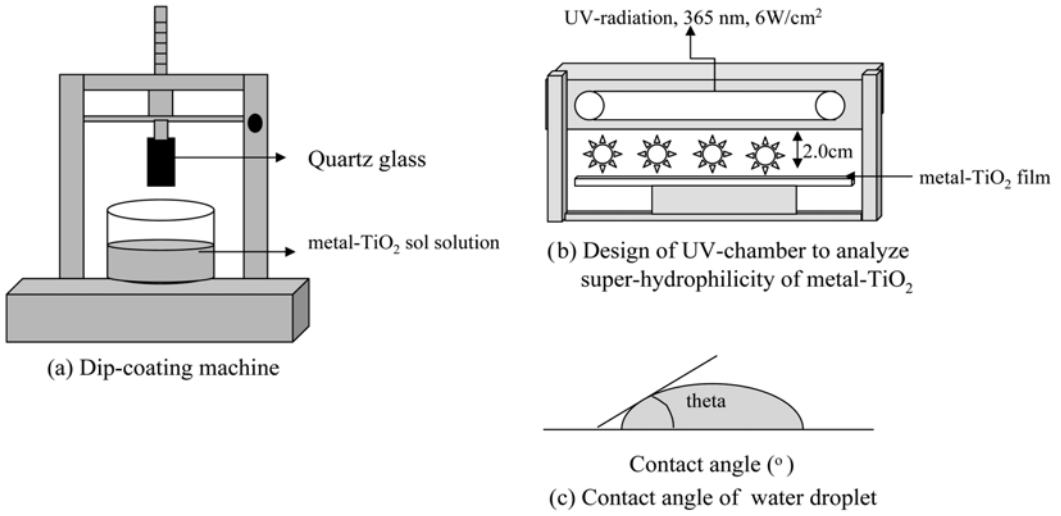

Fig. 2. Fixation of metal-incorporated TiO_2 photocatalysts by using the dipping method and the test of contact angle for water droplets over metal-incorporated TiO_2 films.

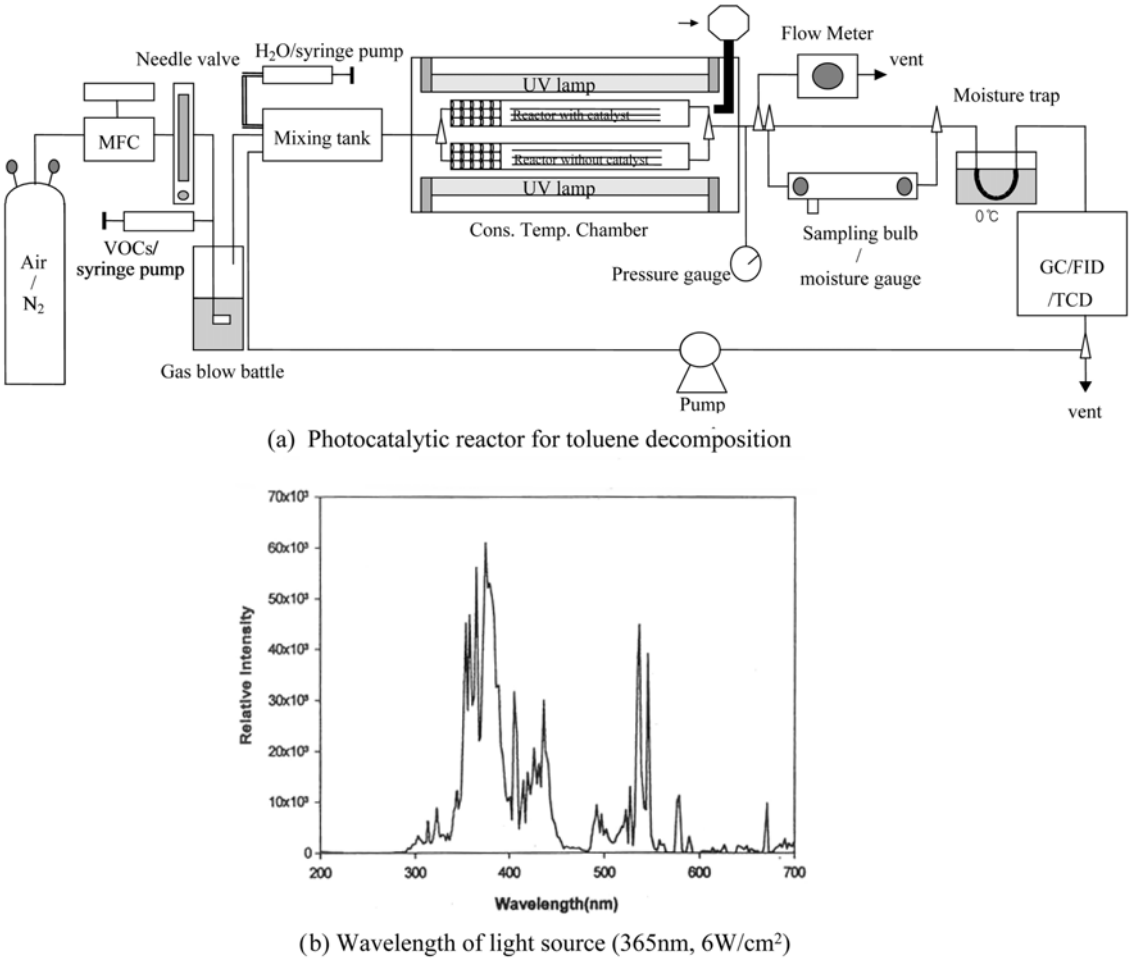

Fig. 3. Photocatalytic reactor for toluene decomposition and wavelength of 365-nm UV light source.

cial contact angle meter (PELCO Inc., model PCHM575-4), allowing for an experimental error of ±1°. For the sake of reliability, the measurement was repeated five times for each sample.

5. Toluene Decomposition on Metal-TiO_2 Photocatalytic System

The decomposition of toluene was carried out by using a continuous reactor as shown in Fig. 3 (a). A quartz cylinder reactor, 15.5 cm long and 1.25 cm in diameter, was used and UV-lamps (model BBL, 365 nm, 24.0(6.0×4ea)W/m^2, 20 cm long×1.5 cm in diameter, Shinan Co., Korea) were used for toluene photodecomposition. Six Pyrex sticks (12.0 cm long, 2 mm in diameter) were placed in the reactor, the total amount of coated catalyst was fixed at 0.05 g,

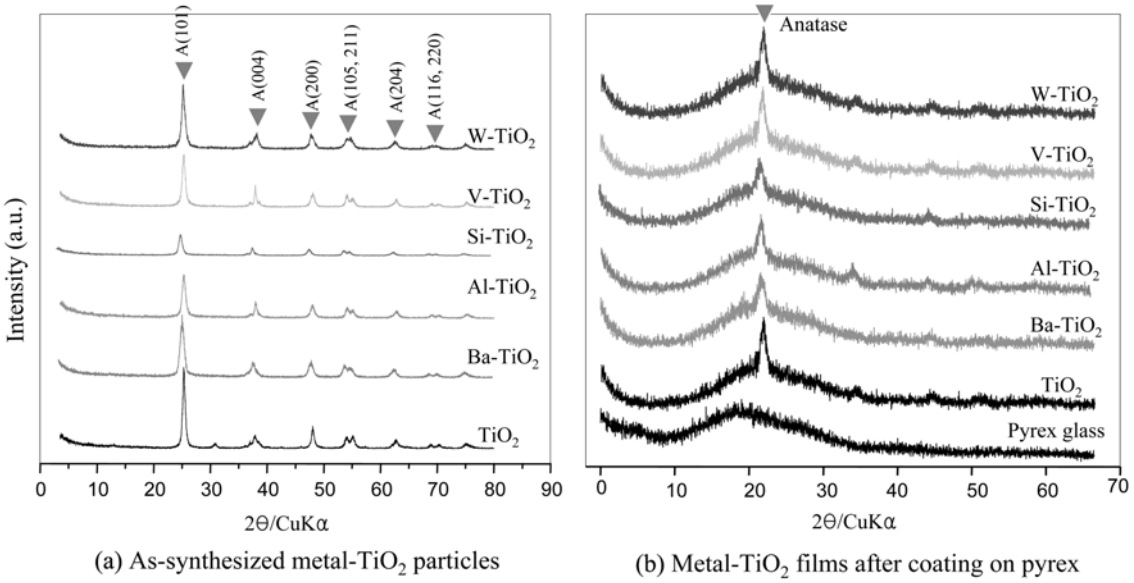

Fig. 4. XRD patterns of particles and films of metal-incorporated TiO_2 photocatalysts prepared by the solvothermal method: a) as-synthesized metal-TiO_2 particles and b) metal-TiO_2 films after coating on Pyrex.

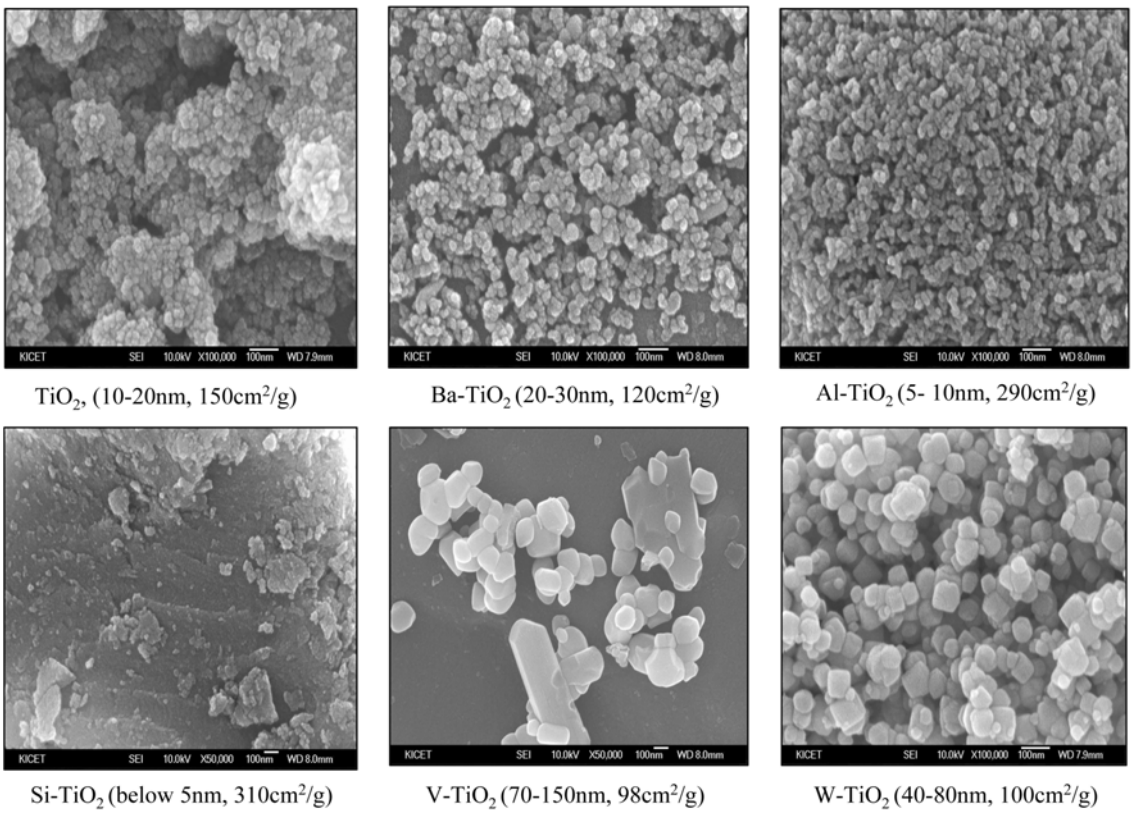

Fig. 5. FESEM images and BET surface areas of metal-incorporated TiO_2 particles prepared by the solvothermal method.

and the toluene concentration was fixed at 100 ppm. In a continuous system, N_2 gas was used as a carrier gas with 100 ppm toluene and an O_2 gas flow rate of 150 mL/min. Added H_2O concentration was fixed to 10.0 wt% per toluene total concentration. The products in the toluene photocatalytic decomposition were analyzed with a TCD and FID-type gas chromatograph (GC) under the following conditions: detector, TCD; column, chromosorb 102; injection temp., 200 °C; initial temp., 40 °C; final temp., 200 °C; and detector temp., 200 °C. The UV-light radiation of the used lamp is shown in Fig. 3 b). The main wavelength was distributed in the range of 300-450 nm.

RESULTS AND DISCUSSION

1. Characterization of Nanometer-sized Metal-TiO_2

Fig. 4 shows the XRD patterns of TiO_2, Ba-TiO_2, Al-TiO_2, Si-TiO_2, V-TiO_2, and W-TiO_2 nanometer-sized powders and films. In general, the TiO_2 photocatalyst with anatase structure was attained in the sol-gel process after the calcination step at 400 °C for 3 h. This structure could, however, also be synthesized in the solvothermal method at 200 °C for 10 h, without any other treatment. The metal-TiO_2 with anatase structure was also attained in this study merely through synthesis by solvothermal treatment at 200 °C. On the other hand, it was well-known that the anatase structure exhibited a higher photocatalytic activity than catalysts of other structures such as rutile, brookite, and amorphous did. All the samples showed well-developed anatase structures (represented by the triangle symbol). In addition, metal-oxides, which presented outside anatase frameworks, were not found. This result indicates that the metal ions of 10.0 wt% were well-inserted into the TiO_2 anatase frameworks. On the other hand, also for metal-TiO_2 films, all samples showed a two-theta value of 25, corresponding to an anatase special peak. This result confirmed that the metal-TiO_2 nano-sized particles were well-fixed on the Pyrex glass substrate.

Fig. 5 shows the FESEM photographs of the particle shape and size distribution of TiO_2 and metal-TiO_2 nano-sized particles. All samples, except V-TiO_2, exhibited relatively spherical types. When Ba^{2+}, Al^{3+}, and Si^{4+} ions were added, the particle sizes decreased to 10-30 nm more than that of pure TiO_2, and in particular, the Si-TiO_2 particles were the smallest. Otherwise, when V and W components were added, the particle sizes increased compared to that of pure TiO_2.

Table 1 summarizes the physical properties of the TiO_2 and metal-TiO_2 photocatalysts. The real metal composition was almost the same as the amount of precursor in the sol preparation, except for V addition. No special peaks of the vanadium oxide were evident in the XRD result, whereas we assumed that V oxides partially remained outside the V-TiO_2 anatase frameworks in the EDS results. On the other hand, while the surface areas were raised with Al and Si ion additions, they were decreased with V and W ion additions. This result was attributed to the particle size determinations from the FESEM results. We also checked the pH values in the metal-TiO_2 colloidal solutions, which were dispersed in DI water, and gained important data. The pH was decreased in all metal-TiO_2 photocatalysts compared to that of pure TiO_2. When Ba, Al, and Si ions were added, the pH was slightly decreased to 6.0-6.36, compared to that of pure TiO_2. However, V and W ion addition greatly increased the acidity to about 4.67-5.25. These results suggested that the surfaces of Ba, Al, and Si-TiO_2, which included the metals of lower oxidation state than Ti^{4+}, slightly attracted the OH- ions, while the surfaces of V-TiO_2 and W-TiO_2, which included the metals of higher oxidation state than Ti^{4+}, more strongly attracted the OH- ions in water. In addition we estimated the zeta-potential value at pH=7.0 (in DI water), with the result that the meta-TiO_2 semiconductors, including the metals of either lower or higher oxidation state than Ti^{4+}, exhibited either negative or positive value, respectively. This result suggested that the surface of meta-TiO_2 semiconductors, which included the metals of either lower or higher oxidation state than Ti^{4+}, was surrounded by either OH^- or H^+ ions, respectively. Therefore, we found that these metal additions may influence the hydrophilicity and photocatalytic activity of metal-TiO_2.

Fig. 6 shows the XPS analysis results for Ti2p and O1s in nano-sized metal-TiO_2 particles. The Gaussian values were used in the curve resolution. In the Ti2p orbital, two peaks also appeared which were assigned to 2p1/2 of low electron density (LUMO) and to 2p3/2 of high electron density (HOMO). In general, the bond occurred between the LUMO orbital of metal and the HOMO orbital of oxygen. The Ti 2p1/2 and Ti 2p3/2 spin-orbital splitting photoelectrons for all the samples were located at the binding energies of about 463.7 eV and 458.1 eV, respectively. With Al and Si ion additions, the Ti2p peaks were slightly shifted to a lower binding energy than that of pure TiO_2, but were shifted to a higher binding energy with V and W ion additions. As is well-known, a higher binding energy indicates a higher oxidized metal state. Therefore, we suggested that the oxidation states of Ti ion in Ba, Al, and Si-TiO_2 were closer to less oxidized states, whereas the Ti states in V and W-TiO_2 were more oxidized than the Ti^{4+} states in pure TiO_2. On the other hand, the O1s region was also split into several contributions. The main contribution was attributed to Ti-O (529.5 ev) in TiO_2, Ti-O (531 ev) in Ti_2O_3 or Ti-OH (hydroxyl group, 531 ev), and adsorbed H_2O (534 ev) [17]. The O1s region was separated into two contributions in

Table 1. Physical properties of particles and films of metal-incorporated TiO_2 photocatalysts prepared by the solvothermal method

Catalysts	Composition on surface (Atomic%)			Surface area (cm^2/g)	Surface resistance ($\Omega/\blacksquare$)	pH in water	Zeta potential in water (mv)
	Me	Ti	O				
TiO_2		25.0	75.00	150	10^{10}	6.40	−28.95
Ba-TiO_2	2.37	23.62	74.02	120	10^{9}	6.01	−21.22
Al-TiO_2	3.31	23.24	73.26	290	10^{10}	6.36	−14.73
Si-TiO_2	2.0	22.16	75.84	310	10^{9}	6.15	−25.60
V-TiO_2	8.79	19.03	72.17	98	10^{8}	4.67	+30.45
W-TiO_2	1.96	25.0	73.04	100	10^{6}	5.25	+20.58

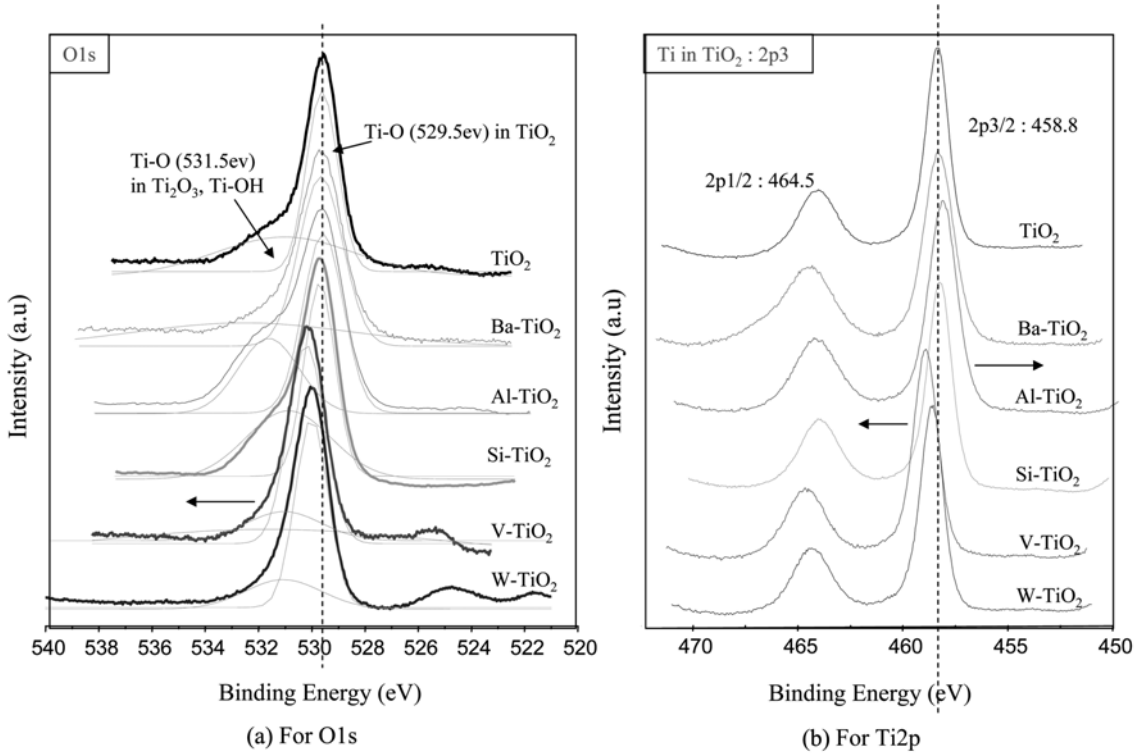

Fig. 6. XPS spectra of metal-incorporated TiO_2 particles prepared by the solvothermal method: a) O1s and b) Ti2p.

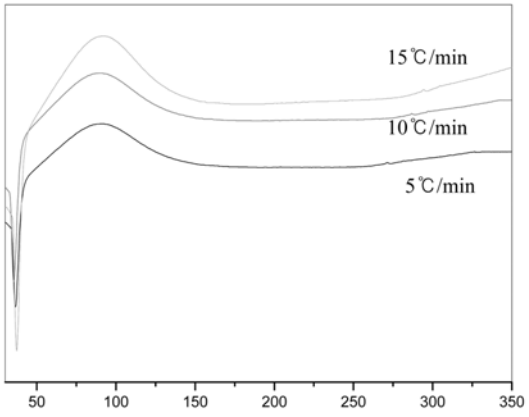

(a) DSC curve of metal-TiO_2 particles

[Ozawa Method]

$$\log\Phi + \frac{0.456E}{RT_m} = \text{constant}$$

Φ = heating rate (℃/min)
R = gas constant
T_m = maximum deflection temperature
E = activation energy

(b) Activation energy and H_2O desorption amount

Catalyst	Activation energy for H_2O desorption by Ozawa' method (kcal/mol)
TiO_2	16
Ba-TiO_2	15
Al-TiO_2	24
Si-TiO_2	20
V-TiO_2	9
W-TiO_2	10

Fig. 7. DSC curve of metal-TiO_2 particles and the activation energy for H_2O desorbed.

this study, which were assigned to the Ti-O and Ti-OH bonds. The peak positions were not shifted in the meta-TiO_2 semiconductors, which included the metals of lower oxidation state than Ti^{4+}, but were shifted to the higher binding energy for the meta-TiO_2 semiconductors, which included the metals of higher oxidation state than Ti^{4+}. In particular, the intensity of Ti-OH, which was related to hy-

drophilicity, increased in the order of Ba-TiO_2>V-TiO_2>W-TiO_2> pure TiO_2>Si-TiO_2>Al-TiO_2. This result confirmed that the hydrophilicity could increase with the addition of Al and Si components to the TiO_2 anatase framework.

Fig. 7 compares the activation energy for dehydration calculated by using Ozawa's method and the DSC curve. Ozawa presented a useful equation to calculate the activation energy. The activation energy value has been used to illustrate the hydrophilic property. In general, higher activation energy corresponds to increased hydrophilicity. The activation energies were higher with Al and Si additions, but lower with V and W additions, as mentioned in the XPS results.

Fig. 8 shows the UV-visible spectra of metal-TiO_2 particles. In general, the absorption of Ti^{4+} tetrahedral symmetry appeared at around 350 nm. The absorption bands of metal-TiO_2 were shifted to slightly shorter wavelengths than those of pure TiO_2. In particular, the Ba-, V-, and W-incorporated TiO_2 particles included the bands assigned to metal ion octahedral symmetries, which were broadly

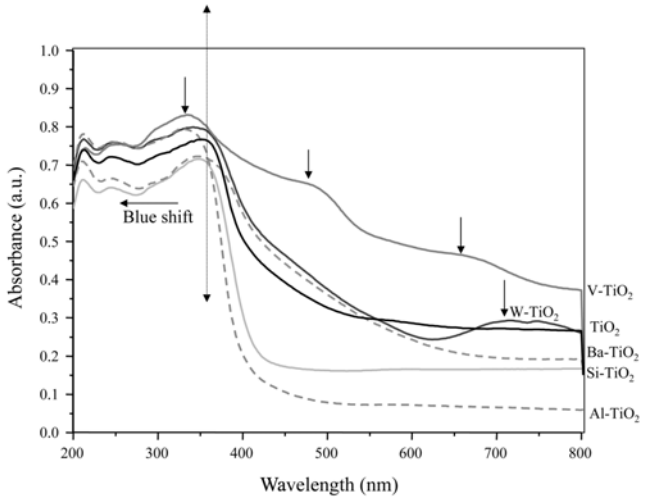

Fig. 8. UV-Visible spectra of metal-incorporated TiO_2 particles prepared by the solvothermal method.

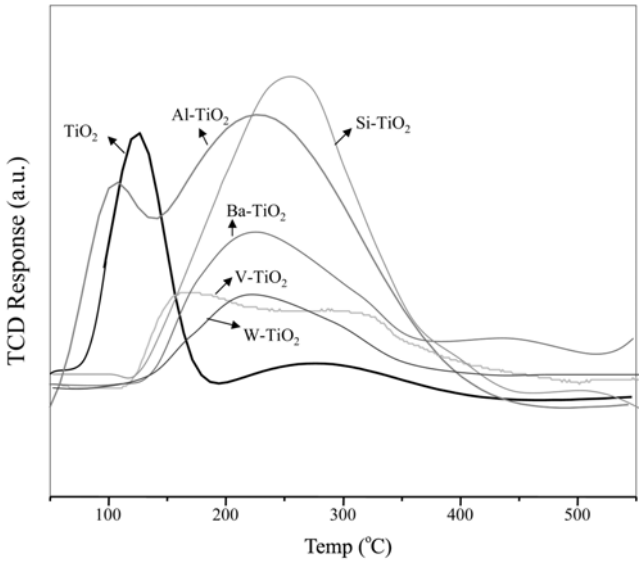

Fig. 9. NH_3-TPD spectra of metal-incorporated TiO_2 particles prepared by the solvothermal method.

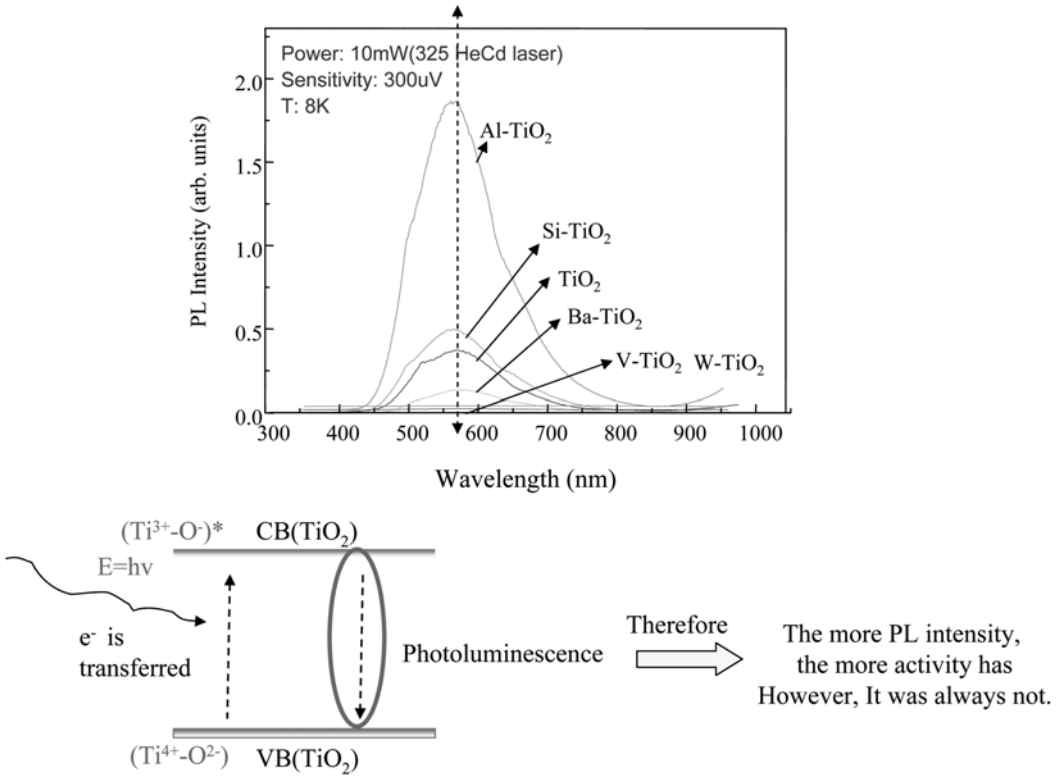

Fig. 10. Photoluminescence (PL) spectra of metal-incorporated TiO_2 particles prepared by the solvothermal method.

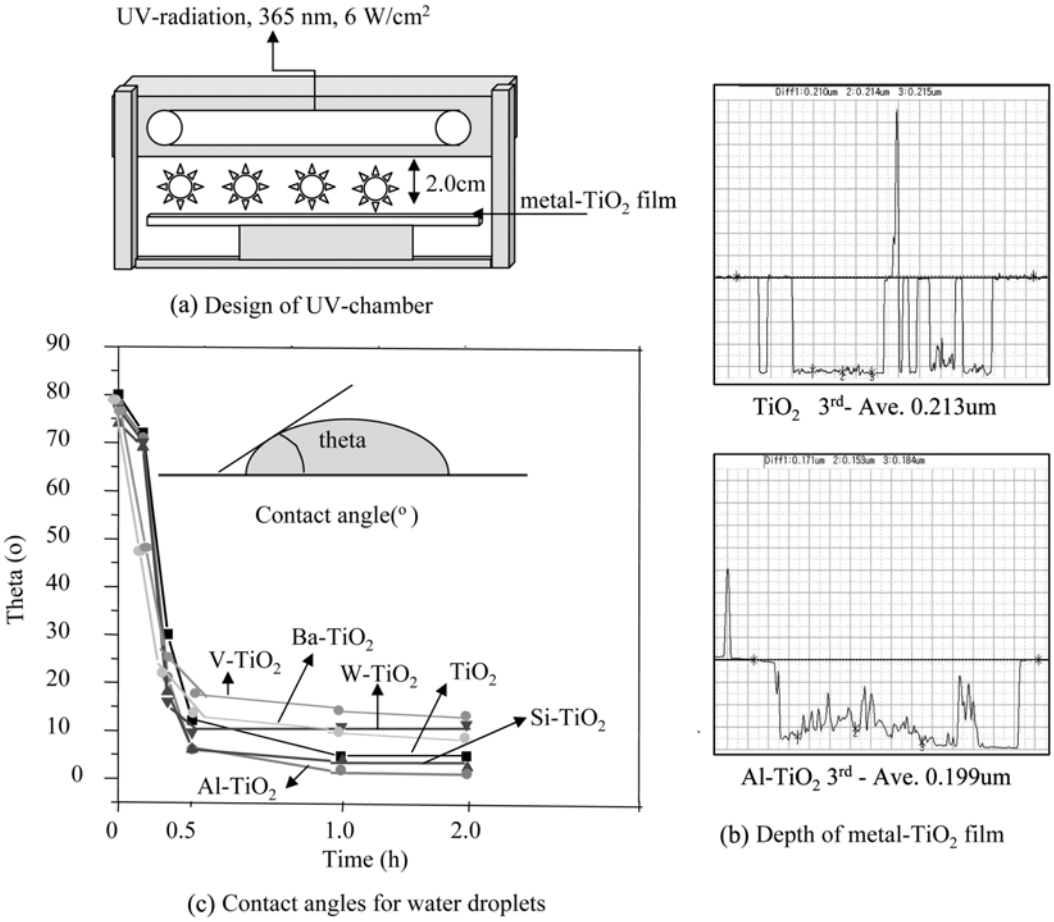

Fig. 11. Contact angles for water droplets on metal-incorporated TiO_2 films prepared by the solvothermal method.

shown as long tails. This indicated that the Ba, V, and W oxide components were physically contacting the external surface of the TiO_2 anatase structure.

To confirm the effect of metal addition into the titanium dioxide framework, we performed the NH_3-TPD test and the profiles are shown in Fig. 9. These profiles consisted of two peaks: one at a low temperature range around 100-150 °C and the other at a high temperature range around 200-300 °C. The low and high temperature peaks corresponded to the weak and strong acid sites, respectively. In the case of pure TiO_2, only one peak assigned to either weak acid sites or H_2O desorption was found, while a second peak around 250 °C was seen in the metal-TiO_2 samples. This result explains that the new acid sites on the TiO_2 framework were generated by the metal additions. In particular, the intensity increased more when the metals of lower, compared to those of higher, oxidation state than Ti^{4+} were added to the TiO_2 frameworks. On the basis of this result, we expect that the generated acidity has been strongly influenced on photo-catalysis for toluene decomposition: the more acidity has the more photo-catalysis.

Fig. 10 shows the PL spectra. Generally, when a semi-conducting material receives external energy, an electron from valence band is transferred to the conduction band, followed by a recombination process of radiation and non-radiation, of which the former can be detected by PL spectroscopy. Consequently, when at high PL values, the photo-activity for VOC decomposition will be increased. However, this relationship was not always observed. In the presence of metals capturing excited electrons or metals with higher conductivity, the PL intensity decreases. In addition, the band shift indicates the decrease of sub-band gap or deep traps. However, the influence of the shift to the right on photo-catalytic performance was not clearly determined. As shown in this figure, band shifts to the right over metal-TiO_2 particles were not found. However, the intensities were decreased in the order of Al-TiO_2<Si-TiO_2<TiO_2< Ba-TiO_2<V-TiO_2<W-TiO_2.

3. Hydrophilicity of Metal-TiO_2 Nanometer-sized Films

Fig. 11 summarizes the change of contact angle for water droplets, i.e., hydrophilicity, on nano-sized, metal-TiO_2 films under UV-irradiation with 365 nm. Generally, hydrophilicity increases with decreased contact angle. Without UV-irradiation, the contact angles exceeded 80° in most samples, but were dramatically decreased under UV-irradiation. Most samples showed below 10° after 2 h, and in particular, the contact angle remarkably dropped to 0° at just 30 min on the Al and Si-TiO_2 films. These results confirmed that the hydrophilicity on the surface of the TiO_2 films was further enhanced by Al or Si ion addition.

4. Toluene Photodecomposition on Metal-TiO_2 Films

Fig. 12 presents the toluene conversions over metal-TiO_2 photocatalyst films with or without H_2O addition in continuous system. Two previous studies have suggested that the optimum H_2O amount is 10.0% by weight per reactant [17,18]. Therefore, 10.0 wt% H_2O

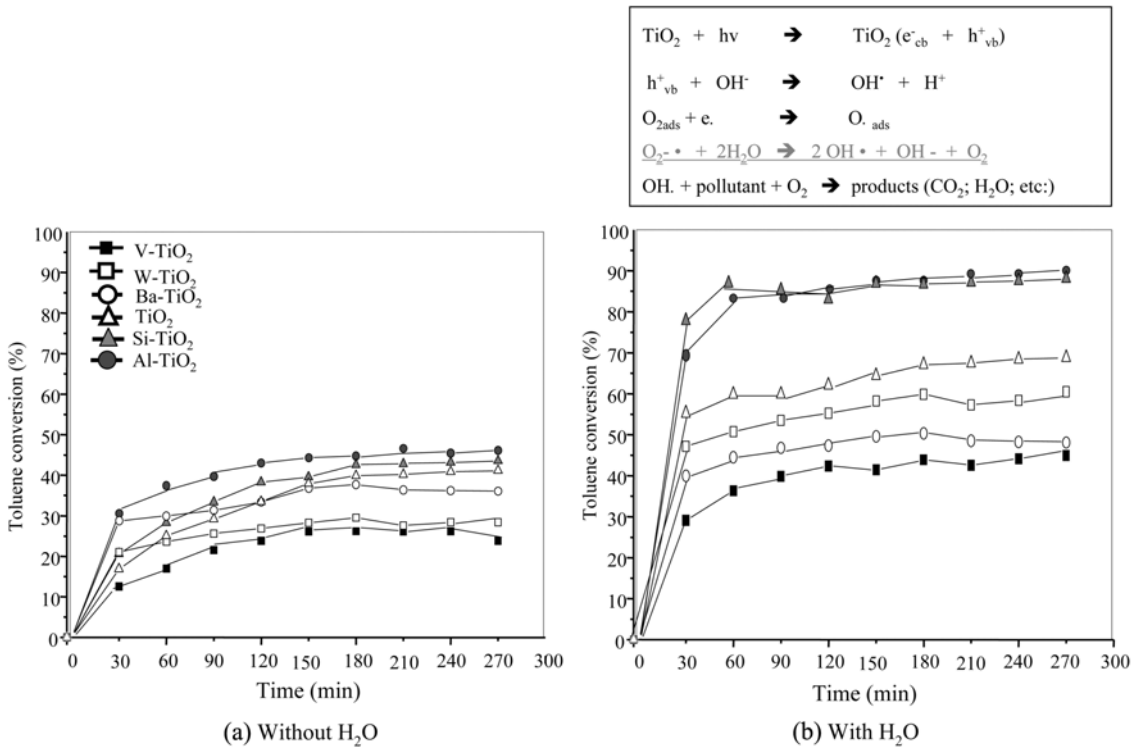

Fig. 12. Toluene photodecomposition on metal-incorporated TiO_2 films, with or without H_2O addition in a batch photo-system, and the mechanism of VOC decomposition with H_2O addition. Reaction conditions: toluene concentration, 100 ppm; catalyst weight, 0.5 g; UV light intensity, 365 nm; 24 W/cm^2; Batch system.

was also used in this study. Without H_2O addition, about 40% of the toluene was decomposed by the pure TiO_2 film after 60 min, after which the conversion continued for a further 24 h. The toluene conversion decreased in the Ba-, V-, and W-TiO_2 films, but increased in the Al-TiO_2 and Si-TiO_2 films by about 45% compared with that of pure TiO_2 film. On the other hand, with the addition of H_2O during the toluene decomposition reaction, the toluene removal rate was remarkably increased in all films. In particular, it reached to 90% in Al-TiO_2 and Si-TiO_2 with increased hydrophilicity. Therefore, this result demonstrates that the hydrophilicity of the photocatalyst positively influences toluene removal. From this result, we suggested that when H_2O is introduced into the toluene decomposition reaction, the activated oxygen, which is generated by a combination of excited electrons and O_2 in the air, attacks the H_2O molecules, to give the generation on the photocatalyst of OH radicals which decompose the toluene. Consequently, we confirmed that hydrophilicity has a strong influence on toluene decomposition, and particularly so when combined with H_2O addition.

After toluene decomposition for 24 h, the consumed metal-TiO_2 photocatalyst was checked and a pale, ash-colored catalyst was found to have been produced in specimens without H_2O addition. Therefore, we conducted C1s XPS analysis to determine whether coke was deposited in the TiO_2 and Al-TiO_2 photocatalysts after toluene photodecomposition, and the result is shown in Fig. 13. In this study, the C1s region was decomposed into several contributions. The main contribution was attributed to isolated C (284.5-285.5 eV), C-N (286.0-287.0 eV) formed in the solvothermal treatment step, and C-O (287.0-290.0 eV) in aldehyde or carbonate. The Gaussian values were used in the curve resolution of the individual C1s peaks. In fresh TiO_2,

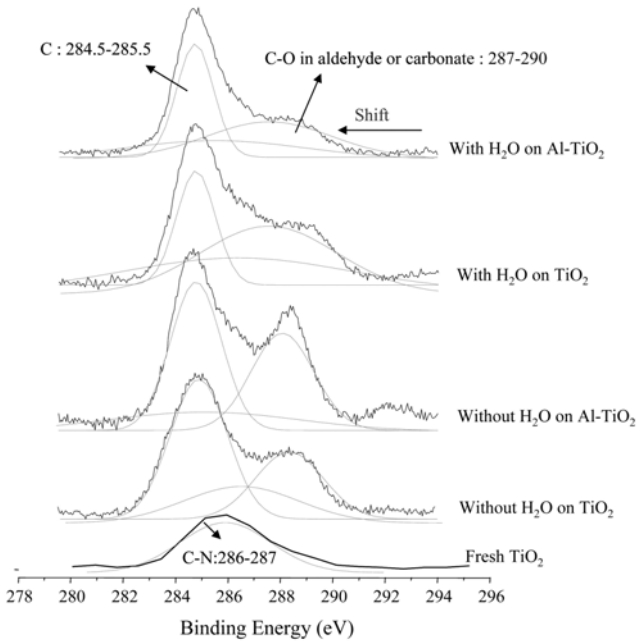

Fig. 13. XPS spectra of C1s orbital for pure or Al-incorporated TiO_2 particles after toluene photo-decomposition reaction.

the C-N peak was just apparent. However, all samples exhibited the C-N, C, and C-O peaks after toluene photodecomposition for 24 h, indicating that the photocatalytic deactivation by deposited carbons could also occur in a similar manner to the thermal cata-

lytic deactivation after VOC photodecomposition. In particular, the C-O peaks increased in both samples without H_2O addition, whereas the C-O and C-N peaks were decreased in both samples with H_2O addition, although the tendency was more remarkable in Al-TiO_2 with increased hydrophilicity. This result confirmed that the photocatalytic deactivation could be retarded by H_2O addition during toluene decomposition reaction, and that, furthermore, this phenomenon had a remarkable effect on the hydrophilic photocatalyst.

CONCLUSION

This study focused on toluene photodecomposition in the presence of H_2O over metal (Ba, Al, Si, V, and W)-incorporated TiO_2. The study results are as follows:

1. The XRD result confirmed the pure anatase structures produced after solvothermal treatment at 200 °C for 24 h, and the metal ions of 10.0 wt% were well incorporated into the anatase framework.

2. The spherical particle sizes were distributed within the range of 20-150 nm, and the particle sizes decreased with the addition of Ba, Al, and Si, featuring oxidation states below 4+, but increased with the addition of V and W, featuring oxidation states above 4+, compared with that of pure TiO_2.

3. The XPS result showed that the Ti-OH peak, which indicates hydrophilicity, increased with increasing Al and Si components, but decreased with increased Ba, V, and W ion components.

4. The contact angle was expressed at about 0-15° on most films (200-nm thick) after irradiation for 2 h, but approached 0° on the Al- and Si-TiO_2 nanometer-sized films after just 30 min.

5. The toluene (100 ppm) photodecomposition in the continuous system increased in the order of Al-TiO_2>Si-TiO_2>pure TiO_2>W-TiO_2>Ba-TiO_2>V-TiO_2, with a maximum toluene conversion rate of 45% being achieved after 120 min. However, the conversion was remarkably increased in all catalysts with H_2O addition during the toluene photo-decomposed reaction, and in particular, the conversion reached up to 90% after 120 min in Al-and Si-TiO_2.

6. After photoreaction, minimal coke was deposited in the photocatalyst in both reaction conditions, with and without H_2O addition. From C1s XPS analysis, it was identified that the deposited amounts were smaller, however, in the reaction with H_2O addition.

Consequently, the hydrophilicity and toluene photodecomposition were more enhanced with the addition of metals with oxidation states lower than 4+, in particular Al or Si ion additions. Furthermore, the hydrophilicity of the photocatalyst had a greater effect on toluene decomposition while the photocatalytic deactivation could be retarded by H_2O supplementation during toluene decomposition.

ACKNOWLEDGEMENTS

This research was supported by a Yeungnam University research grant; No.206-A-054-027, for which the authors are very grateful.

REFERENCES

1. T. H. Lim and S. D. Kim, *Korean J. Chem. Eng.*, **19**, 1072 (2002).
2. M. A. Valenzuela, P. Bosch, J. Jiménez-Becerrill, Q. Quiroz and A. I. Páez, *J. Photochem. & Photobiol. A*, **148**, 177 (2002).
3. Y. Bessekhouad, N. Chaoui, M. Trzpit, N. Ghazzal, D. Robert and J. V. Weber, *J. Photochem. & Photobiol. A*, **183**, 218 (2006).
4. C. Karunakaran and P. Anilkumar, *J. Mol. Catal. A*, **265**, 153 (2007).
5. J. C. Yu, J. Yu, W. Ho and J. Zhao, *J. Photochem. & Photobiol. A*, **148**, 331 (2002).
6. B. Y. Lee, S. H. Park, S. C. Lee, M. Kang, C. H. Park and S. J. Choung, *Korean J. Chem. Eng.*, **20**, 812 (2003).
7. X. Jiang and X. Chen, *J. Crystal Growth*, **270**, 547 (2004).
8. M. Kang and M. H. Lee, *Appl. Catal. A*, **284**, 215 (2005).
9. Q. Liu, X. Wu, B. Wang. and Q. Liu, *Mater. Res. Bull.*, **37**, 2255 (2002).
10. K. Guan, B. Lu and Y. Yin, *Surf. Coat. Tech.*, **173**, 219 (2003).
11. M. Kang, *J. Mol. Catal. A*, **197**, 173 (2003).
12. M. Kang, S. J. Choung and J. Y. Park, *Catal. Today*, **87**, 87 (2003).
13. S. B. Kim, H. T. Hwang and S. C. Hong, *Chemisophere*, **48**, 437 (2002).
14. D. S. Muggli and M. J. Backes, *J. Catal.*, **209**, 105 (2002).
15. M. Kang, S. Y. Lee, C. H. Chung, S. M. Cho, G. Y. Han, B. W. Kim and K. J. Yoon, *J. Photochem. & Photobiol. A*, **144**, 185 (2001).
16. M. Gögebakan and O. Uzun, *J. Mater. Process. Tech.*, **153-154**, 829 (2004).
17. H. J. Choi, J. S. Kim and M. Kang, *Bull. Korean Chem. Soc.*, **28**, 581 (2007).
18. Y. C. Lee Y. P. Hong, H. Y. Lee, H. Kim, Y. J. Jung, K. H. Ko, H. S. Jung and K. S. Hong, *J. Colloid Interf. Sci.*, **267**, 127 (2003).